Data in Brief 48 (2023) 109283

Contents lists available at ScienceDirect

Data in Brief

journal homepage: www.elsevier.com/locate/dib

Data Article

Dataset for the experimental study of dimethyl sulfoxide as a thermodynamic inhibitor of methane hydrate formation

Anton P. Semenov[a,*], Rais I. Mendgaziev[a], Andrey S. Stoporev[a,b]

[a] Gubkin University, Department of Physical and Colloid Chemistry, 65, Leninsky prospekt, Building 1, 119991, Moscow, Russian Federation
[b] Department of Petroleum Engineering, Kazan Federal University, Kremlevskaya str. 18, 420008, Kazan, Russian Federation

ARTICLE INFO

Article history:
Received 31 March 2023
Revised 10 May 2023
Accepted 25 May 2023
Available online 29 May 2023

Dataset link: Raw data of methane hydrate equilibrium / PXRD measurements in system CH4 – H2O – dimethyl sulfoxide and ice freezing points of DMSO aqueous solutions (Original data)

Keywords:
Gas hydrates
Methane
Dimethyl sulfoxide
Thermodynamic hydrate inhibitor
Phase equilibria

ABSTRACT

To determine the ability of dimethyl sulfoxide (DMSO) to inhibit methane hydrate formation by the thermodynamic mechanism, we measured the pressures and temperatures of monovariant equilibrium of three phases: gaseous methane, aqueous DMSO solution, and methane hydrate. A total of 54 equilibrium points were obtained. Hydrate equilibrium conditions have been measured for eight different concentrations of dimethyl sulfoxide ranging from 0 to 55 mass%, at temperatures of 242–289 K and pressures of 3–13 MPa. Measurements were performed in an isochoric autoclave (volume of 600 cm^3, inside diameter of 8.5 cm) at a heating rate of 0.1 K/h and intense fluid agitation (600 rpm) with four-blade impeller (diameter of 6.1 cm, blade height of 2 cm). The specified stirring speed for aqueous DMSO solutions at 273–293 K is equivalent to a range of Reynolds numbers of $5.3 \cdot 10^3$–$3.7 \cdot 10^4$. The endpoint of methane hydrate dissociation at defined temperature and pressure values was taken as the equilibrium point. The anti-hydrate activity of DMSO was analyzed on a mass% and mol% scale. Precise correlations between the thermodynamic inhibition effect of dimethyl sulfoxide ΔT_h and the influencing factors (DMSO concentration and pressure) were derived. Powder X-ray diffractometry was

DOI of original article: 10.1016/j.cej.2021.130227
* Corresponding author.
E-mail address: semenov.a@gubkin.ru (A.P. Semenov).

https://doi.org/10.1016/j.dib.2023.109283

employed to examine the phase composition of the samples at 153 K. Measurement of ice freezing points in aqueous solutions of dimethyl sulfoxide (up to 50 mass%) at ambient pressure allowed us to clarify the location of the liquidus line in the DMSO-H_2O system and to check the hydrate equilibrium data for thermodynamic consistency.

Specifications Table

Subject	Chemistry
Specific subject area	Physical and Theoretical Chemistry
Type of data	Tables, figures
How the data were acquired	Methane hydrate dissociation conditions corresponding to the three-phase V-L_w-H equilibrium have been measured for the CH_4-H_2O-dimethyl sulfoxide (DMSO) system over a broad range of varying factors involving temperature, pressure, and concentration of DMSO in an aqueous solution. The measurements were performed with a constant volume autoclave GHA350 (PSL Systemtechnik, Germany) at a heating rate of 0.1 K/h and intense fluid agitation (600 rpm). The reactor has a volume of 600 cm^3 and an inner diameter of 8.5 cm. The four-blade impeller has a diameter of 6.1 cm and a blade height of 2 cm. The lower edge of the blades is 0.5 cm from the bottom of the reactor. The endpoint of gas hydrate dissociation with defined temperature and pressure values was taken as the equilibrium point in a single test. The amount of liquid aqueous phase to be loaded inside the autoclave for each series at a fixed DMSO concentration was 300 cm^3. At a filling volume of 300 cm^3, the height of the liquid layer in the reactor is 5.3 cm (excluding liquid displacement due to immersion of the stirrer shaft and four-blade impeller) and 6 cm (including the liquid displacement). The GHA350 is instrumented with temperature (Pt100) and pressure sensors as well as an agitation system based on a Hei-TORQUE 400 Precision overhead motor (Heidolph, Germany), a magnetic coupling (Premex, Switzerland), and a four-blade stirrer. The temperature control system consists of an external autoclave jacket with connections for a Ministat 240 thermostat (Huber, Germany) filled with ethanol. The thermostat and sensors of the GHA350 setup are connected to the control PC. After running the script in the WinGHA software, the experiment is executed automatically. The measured values of all parameters are recorded in a log file, which is then used to process the data after the experiment is completed. The phase composition of methane hydrate samples synthesized from aqueous DMSO solutions was analyzed with a D8 Advance diffractometer (Bruker, Germany) coupled to a low-temperature device (Anton Paar, Austria). After synthesis, the hydrate samples were extracted from the autoclave, ground at a temperature of liquid nitrogen, and then placed in a container of the low-temperature device, thermally controlled at 153 K. The ice freezing point of DMSO aqueous solutions was measured employing a calibrated 5622-10-P temperature sensor attached to a 1524 reference thermometer (both Fluke, USA). The sample solution (60 cm^3) was stirred on a magnetic stirrer in a glass cell cooled by circulating ethanol through the F81-ME cryostat (Julabo, Germany). The ice freezing point was taken as the temperature on the plateau after the spike corresponding to the onset of ice crystallization in the supercooled aqueous solution.
Data format	Raw and analyzed
Description of data collection	Methane hydrate dissociation conditions were examined for eight distinct concentrations of dimethyl sulfoxide in solution, including 0, 5.00, 10.00, 20.00, 30.00, 40.00, 50.00, and 55.00 mass%. A total of 54 equilibrium points

(*continued on next page*)

	were obtained. The volume of the liquid phase (aqueous DMSO solution) placed into the autoclave in a single series of experiments was kept constant at 300 cm^3. Thus, the ratio of the free volume to the liquid phase volume in the autoclave was 1:1. The resulting data on the equilibrium conditions of methane hydrate cover the range from 242 to 289 K and from 3 to 13 MPa. Powder X-ray diffraction patterns were obtained for 3 samples of methane hydrate synthesized from aqueous solutions with DMSO mass fractions of 5, 55, and 20 mass%. Ice freezing points were determined at ambient pressure for mass fractions of DMSO in a solution of 0, 5.00, 10.00, 20.00, 30.00, 35.00, 40.00, 45.00, and 50.00 mass%. Considering several replicates, the total number of ice freezing point measurements is 16. The resulting liquidus temperatures for the DMSO-H_2O system are in the range of 227–273 K.
Data source location	Gubkin University, Department of Physical and Colloid Chemistry. Moscow, Russia. 55.692232°N, 37.55487°E
Data accessibility	Repository name: Mendeley Data Data identification number: 10.17632/z4hpjz9t8g.2 Direct URL to data: https://data.mendeley.com/datasets/z4hpjz9t8g
Related research article	A.P. Semenov, R.I. Mendgaziev, A.S. Stoporev, V.A. Istomin, D.V. Sergeeva, A.G. Ogienko, V.A. Vinokurov, The pursuit of a more powerful thermodynamic hydrate inhibitor than methanol. Dimethyl sulfoxide as a case study, Chem. Eng. J. (2021) 130227. https://doi.org/10.1016/j.cej.2021.130227. [1].

Value of the Data

- The derived data on the methane hydrate equilibrium allow quantitative assessment of the anti-hydrate activity of dimethyl sulfoxide as a thermodynamic inhibitor over a wide range of varying factors.
- The data obtained can be useful for predicting the thermodynamic stability of methane hydrate under specified conditions (temperature, pressure, concentration of DMSO).
- The data can be incorporated into the commercial hydrate software for modification and improvement.
- One can apply the data to calculate dimethyl sulfoxide consumption when used as a gas hydrate inhibitor.
- The resulting ice freezing point data clarifies the liquidus line's location in the phase diagram of the DMSO-H_2O system at organic solute concentrations of 0–50 mass%.

1. Objective

The present dataset has been produced by a comprehensive study of the physicochemical properties of DMSO and its aqueous solutions as a possible gas hydrate inhibitor. In order to explore the regularities of methane hydrate inhibition by a thermodynamic mechanism, the three-phase gas-aqueous solution-gas hydrate equilibrium in the CH_4-DMSO-H_2O system was extensively measured within a broad range of dimethyl sulfoxide concentrations (0–55 mass%) and pressures (3–13 MPa). Correlations accurately describing the thermodynamic inhibition of methane hydrate by dimethyl sulfoxide in two different concentration scales (mass% and mol%) within the studied range of factors have been derived from the set of experimental data. The PXRD study of samples synthesized from aqueous DMSO solutions provided new insights into the phase composition of clathrate hydrates formed in the CH_4-DMSO-H_2O system. The diffractograms indicated the formation of sI methane hydrate [1] (non-inclusion of DMSO molecules in the hydrate structure) in the mentioned system. The results of ice freezing point measurements for aqueous DMSO solutions clarified the location of the liquidus line for the DMSO-H_2O system and verified the thermodynamic consistency of the methane hydrate equilibrium data.

2. Data Description

The raw data from the measurements of the methane hydrate equilibrium conditions in the methane-water-dimethyl sulfoxide system are given in the "Hydrate equilibrium (CH_4-DMSO-H_2O)" archive (see https://data.mendeley.com/datasets/z4hpjz9t8g/2). For each of them, there is a separate .xlsx file in the archive with columns of numerical values of the following parameters measured by sensors of the GHA350 autoclave: time, temperature (°C), gauge pressure (bar), stirrer speed (rpm). The file name represents the mass fraction of DMSO in an aqueous phase and the point number. For example, the file "5% DMSO_point 13" corresponds to the raw data for the 13th equilibrium point (numbering from Table 1) for a 5 mass% aqueous solution of dimethyl sulfoxide. Cells D1:F3 of each file display numerical values of the masses and concentrations of the components in the aqueous phase. An example of the $P(T)$-trajectory used to determine the pressure and temperature of the hydrate dissociation endpoint for each measurement is given in the original research paper (see Fig. 1 in ref. [1]). Table 1 contains all obtained numerical values of equilibrium temperatures and pressures of methane hydrate coexisting with aqueous dimethyl sulfoxide solutions (0–55 mass% or 0–22 mol%). For each equilibrium point, hydrate equilibrium temperature suppression ΔT_h was calculated, which characterizes the thermodynamic inhibition effect at a certain equilibrium pressure and shows the temperature shift of the measured equilibrium point relative to the system without DMSO (methane-water). The experimental values of equilibrium temperatures and pressures for all DMSO concentrations are plotted in Fig. 1.

The outcome of the application of the empirical function (Equation 4 from ref. [1]) to get the correlation between the thermodynamic inhibition effect of dimethyl sulfoxide ΔT_h and the influencing factors (DMSO concentration and pressure) is graphically presented in Fig. 2 in the form of a three-dimensional diagram. The derived magnitudes of the correlation parameters for the DMSO anti-hydrate activity in a mass% and mol% scale are summarized in Table 2. The calculated values of ΔT_h, as well as the difference between the experimental and calculated ones for all experimental points, are in Tables 3 and 4 and Fig. 3.

The raw data presented in the archive "PXRD analysis (CH_4-DMSO-H_2O)" are related to the powder X-ray diffraction study of the phase composition of gas hydrate samples synthesized from DMSO aqueous solutions. Diffractograms were recorded for 3 samples with a mass fraction of dimethyl sulfoxide in an aqueous solution of 5, 55, and 20 mass%. For each sample, a separate file containing numerical values of 2θ (degree) and signal intensity (a.u.) is provided. Table 5 presents numerical data on the PXRD of methane hydrate samples obtained from 5, 20, and 55 mass% DMSO solutions. In the case of 20 mass%, preparation was carried out from a frozen solution (see [1] for more detail).

The raw data from the determination of the ice-freezing temperatures of aqueous DMSO solutions at atmospheric pressure are given in the "Ice Freezing (H_2O-DMSO)" archive. The archive contains raw data from sixteen ice freezing point measurements. The file name indicates the mass fraction of DMSO and the point number (see Table 6). Each file has a column with the measured temperature values of the sample at the specified time (one temperature reading every two seconds). The experimental ice freezing points of aqueous DMSO solutions measured in this work are reported in Table 6. The same data are plotted in Fig. 4, along with a polynomial approximation. For comparison, Fig. 4 shows the literature values of the liquidus line temperature for the DMSO-H_2O system [2–5].

Table 1
Methane hydrate dissociation data for CH_4-DMSO-H_2O system (equilibrium temperature *T*, pressure *P*, and suppression of hydrate equilibrium temperature ΔT_h at *P* value relative to uninhibited system with pure H_2O (sample #1)); heating rate near the endpoint of methane hydrate decomposition was 0.1 K/h.

Sample #	DMSO concentration in aqueous solution, mass% [a] (mol%)	Point #	T, K [b]	P, MPa [c]	ΔT_h, K
1	0	1	274.25	2.89	0
		2	276.96	3.79	0
		3	279.26	4.77	0
		4	281.11	5.78	0
		5	282.62	6.77	0
		6	283.87	7.78	0
		7	285.01	8.84	0
		8	286.14	10.03	0
		9	287.03	11.14	0
		10	287.65	12.01	0
		11	287.85	12.32	0
		12	289.02	14.22	0
2	5.00 (1.20)	13	273.69	2.98	0.88
		14	278.78	4.98	0.91
		15	282.19	7.15	0.92
		16	284.73	9.47	0.90
		17	287.39	13.01	0.92
3	10.00 (2.50)	18	272.44	2.92	1.92
		19	277.79	5.01	1.95
		20	281.18	7.18	1.97
		21	283.67	9.48	1.98
		22	286.28	12.97	2.00
4	20.00 (5.45)	23	269.56	2.91	4.77
		24	274.93	4.99	4.77
		25	278.29	7.14	4.81
		26	280.78	9.47	4.85
		27	282.95	12.28	4.89
		28	283.36	12.96	4.91
5	30.00 (8.99)	29	265.52	2.99	9.06
		30	270.55	4.95	9.06
		31	270.61	4.96	9.03
		32	273.66	6.89	9.11
		33	276.53	9.50	9.13
		34	279.08	12.99	9.21
6	40.00 (13.32)	35	258.37	2.90	15.90
		36	258.42	2.91	15.89
		37	263.83	5.00	15.90
		38	267.11	7.14	15.99
		39	269.57	9.47	16.06
		40	272.09	12.92	16.16
7	50.00 (18.74)	41	246.85	3.02	27.84
		42	251.40	4.77	27.85
		43	251.43	4.77	27.84
		44	255.18	7.18	27.97
		45	257.55	9.50	28.11
		46	259.61	12.93	28.65
		47	259.62	12.95	28.65
8	55.00 (21.99)	48	242.41	4.91	37.13
		49	245.03	6.50	37.20
		50	245.74	7.11	37.33
		51	247.95	9.32	37.54
		52	248.82	10.92	38.04
		53	249.83	12.94	38.43
		54	249.78	12.95	38.49

[a] Expanded uncertainty of DMSO mass fraction is 0.012 mass% ($k = 2$).
[b] Expanded uncertainty is 0.1 K ($k = 2$).
[c] Expanded uncertainty is 0.02 MPa ($k = 2$).

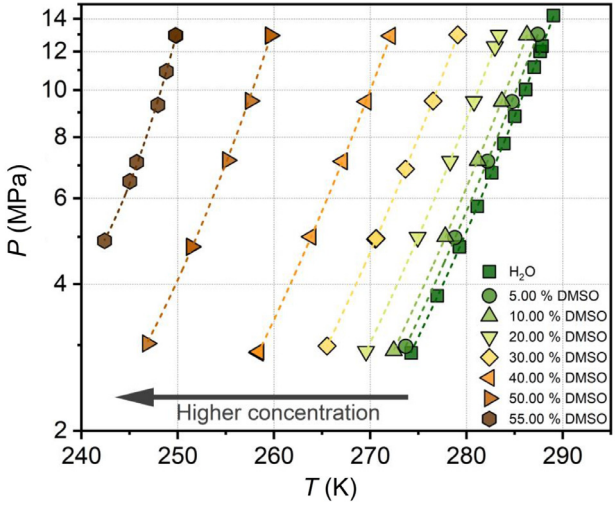

Fig. 1. Measured methane hydrate dissociation points (experiment) for the CH_4-DMSO-H_2O system; dashed color lines are approximations (see Table S2 in the Supplementary of the original research paper [1]) by the three-parameter function $P = \exp(A + B/T + C \ln T)$; legend shows DMSO mass percentage in aqueous solution; error bars are smaller than the size of the symbols.

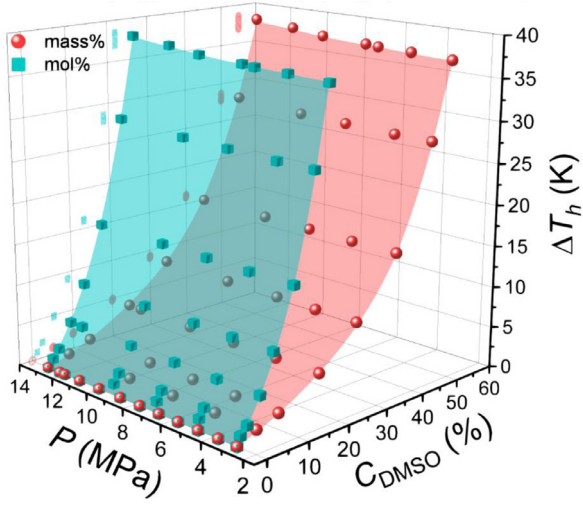

Fig. 2. 3D plots of methane hydrate equilibrium temperature depression ΔT_h vs. DMSO concentration in two scales (mass% and mol%) and pressure, symbols are experimental ΔT_h values, transparent surfaces are fits by empirical equation 4 from ref. [1] (parameters are summarized in Table 2); error bars are smaller than the size of the symbols.

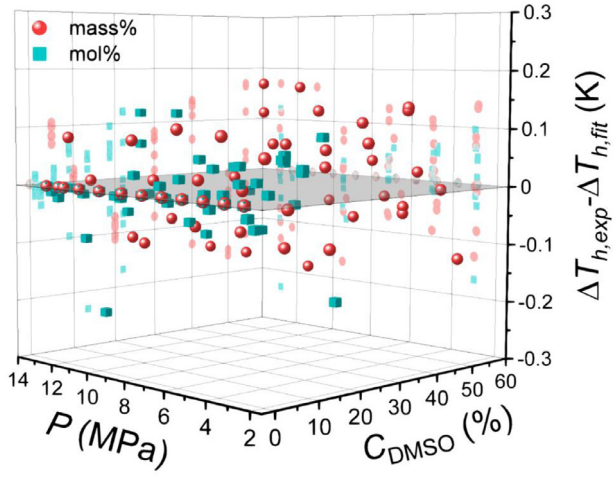

Fig. 3. 3D plot of the difference between the experimental and calculated value of ΔT_h for all experimental points by two approximations in the mass% and mol% scales, the symbols correspond to the residuals in the rightmost column of Tables 3 and 4.

Table 2
Parameters of the empiric function (equation 4 from ref. [1]), describing the inhibition activity of dimethyl sulfoxide in terms of methane hydrate equilibrium temperature suppression ΔT_h (system CH_4-DMSO-H_2O) in the range of DMSO concentration in aqueous solutions of 0–55 mass% or 0–21.99 mol% and pressure of 3–13 MPa.

Coefficient	Mass% scale	Mol% scale
b_1	620.1942569	337.8421721
b_2	48.269136	11.0221815
b_3	-1.3723293	0.3800755
b_4	0.0260514	0.0026296
b_5	$1.9510394 \cdot 10^{-4}$	0.0021344
b_6	$-2.9594138 \cdot 10^{-7}$	$-3.470995 \cdot 10^{-6}$
b_7	$6.0922365 \cdot 10^{-8}$	$6.8334898 \cdot 10^{-7}$
Adjusted R^2	0.99996	0.99998
Average absolute deviation (K)	0.08	0.05
Average absolute relative deviation (%)	1.74	0.52

Table 3
Results of surface fitting by empirical function 4 from ref. [1] of the methane hydrate equilibrium temperature suppression ΔT_h vs. DMSO content in water solution and gas pressure in mass% scale for the CH_4-DMSO-H_2O system.

DMSO mass fraction, mass%	*P*, MPa	ΔT_h experiment, K	ΔT_h fit, K	Residuals of ΔT_h (experiment-fit), K
0	2.89	0	0	0
0	3.79	0	0	0
0	4.77	0	0	0
0	5.78	0	0	0
0	6.77	0	0	0
0	7.78	0	0	0
0	8.84	0	0	0
0	10.03	0	0	0
0	11.14	0	0	0
0	12.01	0	0	0
0	12.32	0	0	0
0	13.01	0	0	0
5.00	2.98	0.88	0.81	0.07
5.00	4.98	0.91	0.81	0.10
5.00	7.15	0.92	0.81	0.11
5.00	9.47	0.90	0.82	0.08
5.00	13.01	0.92	0.84	0.08
10.00	2.92	1.92	1.93	-0.01
10.00	5.01	1.95	1.94	0.01
10.00	7.18	1.97	1.94	0.02
10.00	9.48	1.98	1.96	0.01
10.00	12.97	2.00	2.00	0.00
20.00	2.91	4.77	4.85	-0.08
20.00	4.99	4.77	4.86	-0.09
20.00	7.14	4.81	4.88	-0.07
20.00	9.47	4.85	4.92	-0.07
20.00	12.28	4.89	5.00	-0.11
20.00	12.96	4.91	5.02	-0.10
30.00	2.99	9.06	8.98	0.08
30.00	4.95	9.06	8.99	0.07
30.00	4.96	9.03	9.00	0.04
30.00	6.89	9.11	9.03	0.07
30.00	9.50	9.13	9.12	0.01
30.00	12.99	9.21	9.29	-0.08
40.00	2.90	15.90	15.76	0.14
40.00	2.91	15.89	15.76	0.13
40.00	5.00	15.90	15.79	0.11
40.00	7.14	15.99	15.86	0.13
40.00	9.47	16.06	16.00	0.07
40.00	12.92	16.16	16.30	-0.14
50.00	3.02	27.84	27.84	-0.00
50.00	4.77	27.85	27.89	-0.04
50.00	4.77	27.84	27.89	-0.05
50.00	7.18	27.97	28.04	-0.07
50.00	9.50	28.11	28.28	-0.17
50.00	12.93	28.65	28.80	-0.16
50.00	12.95	28.65	28.81	-0.16
55.00	3.00	36.91	37.04	-0.13
55.00	4.91	37.13	37.11	0.02
55.00	6.50	37.20	37.23	-0.03
55.00	7.11	37.33	37.29	0.03
55.00	9.32	37.54	37.59	-0.05
55.00	10.92	38.04	37.87	0.16
55.00	12.94	38.43	38.32	0.11
55.00	12.95	38.49	38.32	0.17

Table 4
Results of surface fitting by empirical function 4 from ref. [1] of the methane hydrate equilibrium temperature suppression ΔT_h vs. DMSO content in water solution and gas pressure in mol% scale for the CH_4-DMSO-H_2O system.

DMSO mol fraction, mol%	*P*, MPa	ΔT_h experiment, K	ΔT_h fit, K	Residuals of ΔT_h (experiment-fit), K
0	2.89	0	0	0
0	3.79	0	0	0
0	4.77	0	0	0
0	5.78	0	0	0
0	6.77	0	0	0
0	7.78	0	0	0
0	8.84	0	0	0
0	10.03	0	0	0
0	11.14	0	0	0
0	12.01	0	0	0
0	12.32	0	0	0
0	13.01	0	0	0
1.20	2.98	0.88	0.90	-0.02
1.20	4.98	0.91	0.90	0.01
1.20	7.15	0.92	0.90	0.02
1.20	9.47	0.90	0.91	-0.01
1.20	13.01	0.92	0.93	-0.01
2.50	2.92	1.92	1.96	-0.04
2.50	5.01	1.95	1.96	-0.01
2.50	7.18	1.97	1.97	-0.00
2.50	9.48	1.98	1.99	-0.01
2.50	12.97	2.00	2.03	-0.02
5.45	2.91	4.77	4.76	0.01
5.45	4.99	4.77	4.76	0.01
5.45	7.14	4.81	4.79	0.02
5.45	9.47	4.85	4.83	0.03
5.45	12.28	4.89	4.90	-0.01
5.45	12.96	4.91	4.92	-0.01
8.99	2.99	9.06	9.00	0.06
8.99	4.95	9.06	9.01	0.05
8.99	4.96	9.03	9.01	0.02
8.99	6.89	9.11	9.05	0.06
8.99	9.50	9.13	9.14	-0.01
8.99	12.99	9.21	9.31	-0.10
13.32	2.90	15.90	15.85	0.05
13.32	2.91	15.89	15.85	0.04
13.32	5.00	15.90	15.88	0.02
13.32	7.14	15.99	15.95	0.04
13.32	9.47	16.06	16.09	-0.03
13.32	12.92	16.16	16.39	-0.23
18.74	3.02	27.84	27.74	0.10
18.74	4.77	27.85	27.79	0.06
18.74	4.77	27.84	27.79	0.05
18.74	7.18	27.97	27.93	0.04
18.74	9.50	28.11	28.17	-0.06
18.74	12.93	28.65	28.70	-0.06
18.74	12.95	28.65	28.71	-0.06
21.99	3.00	36.91	37.08	-0.17
21.99	4.91	37.13	37.15	-0.02
21.99	6.50	37.20	37.27	-0.07
21.99	7.11	37.33	37.33	-0.00
21.99	9.32	37.54	37.63	-0.08
21.99	10.92	38.04	37.92	0.12
21.99	12.94	38.43	38.37	0.07
21.99	12.95	38.49	38.37	0.12

Table 5
PXRD data for methane hydrate samples obtained from aqueous DMSO solutions. The data were acquired at 153 K.

5 mass% DMSO	55 mass% DMSO	20 mass% DMSO	Calculated data on sI methane hydrate and ice I*h* *	
$2\theta_{exp}$ / °			$2\theta_{calc}$ / °	hkl/phase
10.517	–	10.569	10.540	011/sI [a]
14.932	–	14.941	14.927	200/sI
16.707	16.696	16.711	16.700	201/sI
18.288	18.277	18.313	18.307	112/sI
22.804	22.810	22.810	22.813	010/I*h* [b]
24.307	24.273	24.295	24.291	002/I*h*
25.884	25.909	25.930	25.889	011/I*h*
27.077	27.061	27.078	27.085	302/sI
28.106	28.103	28.112	28.128	213/sI
30.098	–	30.104	30.114	400/sI
31.031	31.025	31.051	31.064	104/sI
31.965	–	31.971	31.988	033/114/sI
34.602	–	34.608	34.629	412/sI
–	–	35.437	35.471	323/sI

[a] $Pm\bar{3}n$ cubic structure I.
[b] $P6_3/mmc$ hexagonal ice.* See the Experimental design, materials, and methods section for details.

Table 6
Measured ice freezing points T_{ice} at 0.1 MPa for aqueous solutions of dimethyl sulfoxide; each freezing point given corresponds to a single measurement.

Sample #	DMSO concentration in aqueous solution, mass%	Point #	T_{ice} /°C	T_{ice} / K	ΔT_{ice} / K
I	0	1	0.00	273.15	0
II	5.00	2	-1.34	271.81	1.34
		3	-1.34	271.81	1.34
III	10.00	4	-2.95	270.21	2.94
		5	-2.94	270.21	2.94
IV	20.00	6	-7.14	266.01	7.14
		7	-7.14	266.01	7.14
V	30.00	8	-13.86	259.29	13.86
		9	-13.88	259.27	13.88
VI	35.00	10	-18.75	254.40	18.75
		11	-18.73	254.42	18.73
VII	40.00	12	-25.02	248.13	25.02
		13	-25.04	248.11	25.04
VIII	45.00	14	-34.20	238.95	34.20
		15	-34.19	238.96	34.19
IX	50.00	16	-46.47	226.68	46.47

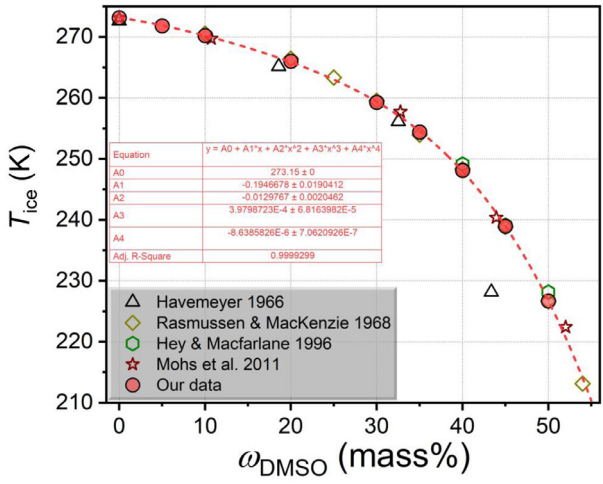

Fig. 4. Ice freezing points of DMSO aqueous solutions at 0.1 MPa (symbols are values measured in this work and literature data [2–5]; the dashed line is the fourth-degree polynomial approximation based on our experimental data); error bars are smaller than the size of the symbols.

3. Experimental Design, Materials and Methods

High-purity methane (>99.99 vol%), purchased from the Moscow Gas Processing Plant (Moscow Region, Russia) in 40 L cylinders at 15 MPa pressure, was used as the hydrate-forming gas. Aqueous solutions were made by using 18.2 MΩ·cm deionized water produced in the laboratory via Simplicity UV (Millipore, USA), and dimethyl sulfoxide qualified as "chemically pure" (>99.8 mass%), received from the ECOS-1 company (Moscow, Russia). To verify the purity, the refractive index of DMSO at the sodium D-line was measured in our laboratory with Abbemat 650 refractometer (Anton Paar, Austria) and amounted to 1.479376 ± 0.000001 at 293.15 K.

Aqueous solutions were prepared by a gravimetric technique by sequentially dosing the components in a glass flask in the amount necessary to achieve the desired concentration of DMSO. The masses of water and dimethyl sulfoxide were metered with a resolution of 0.001 g using PA413C balance (Ohaus Pioneer, USA) with a maximum error not exceeding ± 0.01 g. The amount of aqueous solution sample for methane hydrate measurements was 300–318 g and a fixed volume of 300 cm^3 (since the DMSO solutions have different densities; see Supplementary of ref. [1]).

Gas hydrate equilibrium measurements were conducted utilizing a GHA350 (PSL Systemtechnik, Germany) in a 600 cm^3 constant volume autoclave (an inner diameter of 8.5 cm) at a heating rate of 0.1 K/h and intense agitation of the fluids (600 rpm). The GHA350 is equipped with temperature (Pt100, accuracy ±0.1 K) and pressure (accuracy ±0.02 MPa) sensors and a stirring mechanism based on a Hei-TORQUE 400 Precision overhead motor (Heidolph, Germany), a magnetic coupling (Premex, Switzerland), and a stirring unit with four blades on the shaft. The four-blade impeller has a diameter of 6.1 cm and a blade height of 2 cm. The lower edge of the blades is 0.5 cm from the bottom of the reactor. The temperature control system is an external autoclave jacket with connections for a Ministat 240 thermostat (Huber, Germany) filled with ethanol. The thermostat can keep the coolant temperature stable within ± 0.02 K. 300 cm^3 of DMSO solution was introduced into a GHA350 high-pressure chamber. This filling volume equals the height of the liquid layer in the reactor of 5.3 cm (excluding liquid displacement due to immersion of the stirrer shaft and four-blade impeller) and 6 cm (including liquid displacement). The empty space of the vessel was purged thrice with gaseous methane. Measurements of hydrate equilibria were performed according to the technique previously analyzed in detail [6]. The validity of this technique has been confirmed for various systems with thermodynamic in-

hibitors such as DMSO [7,8], urea [9], methanol [10,11], and glycols [12]. The coordinates of the equilibrium point in each experiment were the pressure and temperature of the complete dissociation of methane hydrate under ramp heating at a slow rate of 0.1 K/h. At this point, there was a drastic decrease in the $P(T)$-trajectory slope during isochoric ramp heating.

We evaluated the flow regime in the autoclave during the operation of the stirring system [13,14]. Reynolds numbers were calculated for aqueous DMSO solutions (0–55 mass%), considering density and viscosity data (see supplementary to the original research paper [1]) and the geometric characteristics of the stirrer. A stirring speed of 600 rpm for aqueous DMSO solutions at 273–293 K yields a range of Reynolds numbers of $5.3 \cdot 10^3$–$3.7 \cdot 10^4$.

The phase composition of methane hydrate samples synthesized from aqueous DMSO solutions was analyzed with a diffractometer D8 Advance (Bruker, Germany) coupled to a low-temperature device (Anton Paar, Austria). Methane hydrate samples were obtained under quiescent conditions at 10.4 MPa and temperatures of 275 K (for 5 mass% DMSO) and 238 K (for 55 mass% DMSO), corresponding to the same 10 K supercooling for the two concentrations of dimethyl sulfoxide. In the case of the 20 mass% DMSO sample, methane hydrate was obtained from an aqueous solution previously frozen and ground at liquid nitrogen temperature. The frozen powder of the DMSO solution was then heated and held in a methane atmosphere at 274 K and 10.4 MPa. After synthesis, the hydrate sample was extracted from the autoclave, ground at the temperature of liquid nitrogen, and then placed in a container of low-temperature apparatus, thermally controlled at 153 K. Diffractograms of the samples were recorded at a constant temperature of 153 K. Hexagonal ice reflections present in all patterns were used as an internal standard. Thus, the positions of the hydrate reflections were corrected, considering the shift in the ice peaks positions. The calculated values ($2\theta_{calc}$) were determined based on the unit cell parameters of ice [15] and methane hydrate [16] at a given temperature.

The freezing point temperatures of aqueous solutions were determined in an 80 cm^3 double-walled glass cell with lateral outlets for connection to an F81-ME cryostat (Julabo, Germany). The sample solution was continuously stirred on a magnetic stirrer at 600 rpm during the measurements using a PTFE-coated stirring rod. The sample temperature was monitored using a calibrated fast-response probe PRT 5622-10-P (Fluke, USA) connected to a 1524 reference thermometer (Fluke, USA). This combination of instruments allows the temperature to be measured with an error of no more than $\pm$ 0.04 K. The coolant temperature was reduced in increments of 1 K; the sample was held for at least 10 min at each step. The ice freezing point was determined as the plateau temperature after the spike representing the onset of ice crystal formation in a supercooled aqueous solution.

Ethics Statements

The studies described in the manuscript adhered to Ethics in publishing standards (https://www.elsevier.com/journals/data-in-brief/2352-3409/guide-for-authors) and did not involve human or animal subjects.

Declaration of Competing Interests

The authors declare that they have no known competing financial interests or personal relationships that could have appeared to influence the work reported in this paper.

Data Availability

Raw data of methane hydrate equilibrium / PXRD measurements in system CH4 – H2O – dimethyl sulfoxide and ice freezing points of DMSO aqueous solutions (Original data) (Mendeley Data).

CRediT Author Statement

Anton P. Semenov: Data curation, Visualization, Writing – original draft, Validation, Writing – review & editing, Project administration, Funding acquisition; **Rais I. Mendgaziev:** Investigation, Data curation; **Andrey S. Stoporev:** Investigation, Visualization, Writing – original draft, Writing – review & editing.

Acknowledgment

This work was supported by the Russian Science Foundation (grant 20-79-10377).

References

[1] A.P. Semenov, R.I. Mendgaziev, A.S. Stoporev, V.A. Istomin, D.V. Sergeeva, A.G. Ogienko, V.A. Vinokurov, The pursuit of a more powerful thermodynamic hydrate inhibitor than methanol. Dimethyl sulfoxide as a case study, Chem. Eng. J. (2021) 130227, doi:10.1016/j.cej.2021.130227.
[2] R.N. Havemeyer, Freezing point curve of dimethyl sulfoxide—water solutions, J. Pharm. Sci. 55 (1966) 851–853, doi:10.1002/jps.2600550822.
[3] D.H. Rasmussen, A.P. Mackenzie, Phase diagram for the system water–dimethylsulphoxide, Nature 220 (1968) 1315–1317, doi:10.1038/2201315a0.
[4] J.M. Hey, D.R. Macfarlane, Crystallization of ice in aqueous solutions of glycerol and dimethyl sulfoxide. 1. A comparison of mechanisms, Cryobiology 33 (1996) 205–216, doi:10.1006/cryo.1996.0021.
[5] A. Mohs, S. Decker, J. Gmehling, The solid–liquid equilibrium of the binary system H2O–DMSO and the influence of a salt (NaCl, KCl) on the thermodynamic behavior, Fluid Phase Equilib. 304 (2011) 12–20, doi:10.1016/j.fluid.2011.01.026.
[6] A. Semenov, R. Mendgaziev, T. Tulegenov, A. Stoporev, Analysis of the techniques for measuring the equilibrium conditions of gas hydrates formation, Chem. Technol. Fuels Oils. 58 (2022) 628–636, doi:10.1007/s10553-022-01429-w.
[7] A.P. Semenov, R.I. Mendgaziev, A.S. Stoporev, V.A. Istomin, D.V. Sergeeva, T.B. Tulegenov, V.A. Vinokurov, Dimethyl sulfoxide as a novel thermodynamic inhibitor of carbon dioxide hydrate formation, Chem. Eng. Sci. 255 (2022) 117670, doi:10.1016/j.ces.2022.117670.
[8] A.P. Semenov, R.I. Mendgaziev, A.S. Stoporev, V.A. Istomin, D.V. Sergeeva, T.B. Tulegenov, V.A. Vinokurov, Dataset for the dimethyl sulfoxide as a novel thermodynamic inhibitor of carbon dioxide hydrate formation, Data Br 42 (2022) 108289, doi:10.1016/j.dib.2022.108289.
[9] Y. Gong, R.I. Mendgaziev, W. Hu, Y. Li, Z. Li, A.S. Stoporev, A. Yu. Manakov, V.A. Vinokurov, T. Li, A.P. Semenov, Urea as a green thermodynamic inhibitor of sII gas hydrates, Chem. Eng. J. (2022) 132386, doi:10.1016/j.cej.2021.132386.
[10] M.B. Yarakhmedov, A.P. Semenov, A.S. Stoporev, Effect of lower alcohols on the formation of methane hydrate at temperatures below the ice melting point, Chem. Technol. Fuels Oils. 58 (2023) 962–966, doi:10.1007/s10553-023-01476-x.
[11] A.P. Semenov, Y. Gong, V.I. Medvedev, A.S. Stoporev, V.A. Istomin, V.A. Vinokurov, T. Li, New insights into methane hydrate inhibition with blends of vinyl lactam polymer and methanol, monoethylene glycol, or diethylene glycol as hybrid inhibitors, Chem. Eng. Sci. 268 (2023) 118387, doi:10.1016/j.ces.2022.118387.
[12] A.P. Semenov, Y. Gong, V.I. Medvedev, A.S. Stoporev, V.A. Istomin, V.A. Vinokurov, T. Li, Dataset for the new insights into methane hydrate inhibition with blends of vinyl lactam polymer and methanol, monoethylene glycol, or diethylene glycol as hybrid inhibitors, Data Br 46 (2023) 108892, doi:10.1016/j.dib.2023.108892.
[13] F. Filarsky, M. Hagelstein, H.J. Schultz, Influence of different stirring setups on mass transport, gas hydrate formation, and scale transfer concepts for technical gas hydrate applications, Appl. Res. 2 (2023), doi:10.1002/appl.202200050.
[14] F. Filarsky, J. Wieser, H.J. Schultz, Rapid Gas hydrate formation—evaluation of three reactor concepts and feasibility study, Molecules 26 (2021) 3615, doi:10.3390/molecules26123615.
[15] K. Röttger, A. Endriss, J. Ihringer, S. Doyle, W.F. Kuhs, Lattice constants and thermal expansion of H_2O and D_2O ice Ih between 10 and 265 K, Acta Crystallogr. Sect. B. 50 (1994) 644–648, doi:10.1107/S0108768194004933.
[16] A.Y. Manakov, O.M. Khlystov, A. Hachikubo, K. Minami, S. Yamashita, A. Khabuev, A.G. Ogienko, A.V. Ildyakov, G.V. Kalmychkov, T.V. Rodionova, Structural studies of lake baikal natural gas hydrates, J. Struct. Chem. 60 (2019) 1437–1455, doi:10.1134/S0022476619090087.